



Dynamic Aperture Studies for HL-LHC with beam-beam effects

D. Banfi, J. Barranco Garcia (EPF, Lausanne Switzerland)

T. Pieloni, (CERN, Geneva, Switzerland now EPF, Lausanne Switzerland)

Abstract

Various possible operational scenarios are foreseen for the High Luminosity Large Hadron Collider (HL-LHC). In this note we summarize the study and characterization of the beam-beam effects for various possible operational scenarios for the High Luminosity Large Hadron Collider (HL-LHC). As an out-come of the study an optimum operational scenario for the HL-LHC is proposed based on dynamic aperture studies and reducing to the minimum the impact of the non-low beta insertions known as the experiments LHCb and ALICE. The impact of the magnets multipolar errors together with other non-linearities is quantified. The Dynamical Aperture (DA) results are used to determine the stability thresholds, while Frequency Map Analysis (FMA) is used to better understand the physical mechanisms. A description of the modification to the Sixtrack code to model the HL-LHC scenarios are also described.

Keywords: Accelerator Physics, Beam-Beam effects, HL-LHC, Dynamic Aperture, Luminosity

Contents

1	Round optics	2
1.1	Beam Beam interactions	2
1.2	Crab crossing	3
1.3	Crossing angle scan	4
1.4	Intensity scan	7
1.5	Errors	8
1.6	β^* leveling	12
1.7	IP8 and IP2 impact and settings	14
2	HL-LHC Weak-Strong Beam-Beam studies summary	18
3	Acknowledgements	18
4	References	20
A	Technical details	22
B	Simulation tools development and checks	23

The High Luminosity upgrade of the Large Hadron Collider (HL LHC) aims at achieving a peak luminosity of $5 \times 10^{34} \text{ cm}^{-2} \text{ s}^{-1}$ with leveling allowing an integrated luminosity of 250 fb^{-1} , enabling the goal of 3000 fb^{-1} in its 10-12 years of lifetime [1].

This can be achieved by colliding $2.2 \cdot 10^{11}$ protons per bunch at a finite crossing angle of $590 \mu\text{rad}$ to avoid parasitic encounters left and right of each experiment. The luminosity reduction due to the crossing angle is estimated to be around 70%, it is therefore foreseen to compensate this loss by the use of crab cavities [1]. The HL-LHC operation at low β^* is possible thanks to the ATS scheme [2]. The corresponding peak luminosity would exceed the $5 \times 10^{34} \text{ cm}^{-2} \text{ s}^{-1}$ therefore an optimal strategy for the leveling is also studied. Results have been published in [3, 4].

The Dynamic Aperture (DA) is defined as the maximum transverse amplitude where the particles perform stable motion, in this studies we compute the region where particle motion is stable over 10^6 turns which is the maximum achievable computation length. Even if the DA does not provide information regarding the emittance growths, it is an important indicator to predict the beam lifetimes imposed by the nonlinear beam dynamics at collision. In the LHC collider the use of DA simulations is very important to define the margins needed in units of beam RMS size when changing the beam properties (e.g. beam charge and emittances) and machine optics (e.g. crossing angle and β^*). In Table 1 we summarize the HL-LHC beam parameters and compare to the LHC nominal design values and the operational parameters of the 2012 physics run.

All simulations are done using the Sixtrack code and SixDesk environment [5], with the optics version SLHCV3.1b and HLLHCV1.0. Except where stated differently, studies are performed without beam-beam interactions in IP 2 and IP8. Since HL-LHC is expected to make use of a full crabbing scheme at the two main experiments (ATLAS and CMS), this feature has been introduced in the Sixtrack code and the impact of such crab crossing is evaluated. The impact of the two low luminosity experiments IP2 and IP8 in different configurations are evaluated in their specific section.

All the simulation shown are relative to the beam-beam 6D kick computed with the Hirata formalism with energy change [6]. The Hirata 6D formalism has been chosen as the baseline for beam-beam studies since it is the model which better describes the beam-beam interactions in the HL-LHC scenarios and because respect to the 4D Bassetti-Erskine formalism [7], used for the LHC design, it has been shown to be the most conservative when evaluating the dynamical aperture.

Table 1: HL-LHC, LHC nominal and LHC 2012 operational parameters

Parameter	LHC Nom	LHC 2012	HL-LHC
$N_p(10^{11} \text{ p/b})$	1.15	1.65	2.2
N_b	2808	1380	2808
Spacing (ns)	25	50	25
ϵ (μrad)	3.75	2.2-2.5	2.5
β^* (m)	0.55	0.6	0.15
α μrad	285	290	590
Q_x	64.31	64.31	60.31
Q_y	59.32	59.32	62.32
ξ_{bb}/IP	0.0034	0.007	0.0033(0.011 cc)

We defined as a solid criterion that the minimum DA should be bigger than 6σ : this value have been chosen as a minimum requirement as in the LHC design Report [8, 9] strategy and also as experimentally proved to be a robust assumption in terms of stability and lifetimes during the LHC 2012 and 2015 experiments [10]. A dynamic aperture of 6σ gives a margin from the chaotic limit which has been identified in the LHC to be at a DA of roughly 4σ or below [11]. When the DA reaches this value the beams and luminosity lifetimes drop drastically to 4-8 hours and important losses have been observed [12]. The HL-LHC assumes beam lifetimes of 12 hours to achieve the designed performances. The rationale behind this assumption is to keep losses due to beam-beam interactions smaller than the burn off of protons due to proton inelastic scattering at the IPs. The expected lifetimes due to burn off is estimated to be of approximately 12 hours considering 2 head-on collisions and an inelastic cross section

of 81 mb . It is therefore fundamental to guarantee at a design stage some margins in the presence of beam-beam interactions. The studies were also performed in parallel with a continuous benchmark with another model Lifetrac used for the modelling of the Tevatron collider and comparisons can be found in [13] and in the final results of the HL-LHC baselines for the Design Report in [4]. The impact of octupoles and the machine chromaticity are not covered in this note but can be found in [14].

1 Round optics

To achieve the high luminosity goals the HL-LHC project relies on very small beta functions at the interaction points. This is possible only using the ATS scheme [2] that will allow to reach β^* as small as 10 cm . During the study different optics have been used and details of the relative files and simulation setup are show in Appendix A. The HL-LHC also relies on crab cavities to compensate for the huge geometric loss factor and needs to keep the luminosity levelled at $5 \cdot 10^{34} \text{ cm}^{-1} \text{ s}^{-1}$ to avoid high pile-up in the experiments.

1.1 Beam Beam interactions

The HL-LHC as the LHC will experience two type of beam-beam effects: the head-on collisions at the main Interaction Points (IPs) corresponding to the ATLAS, CMS, LHCb and Alice experiments and several Long-Range (LR) encounters left and right of the head-on collisions. To avoid long range encounters a minimum separation is needed and this is one of the main outcomes of this study. The beam-beam long range separation at the first parasitic encounter is for the high luminosity experiments, ATLAS and CMS, defined as:

$$d_{sep} = \alpha \cdot \sqrt{\frac{\beta^* \cdot \gamma}{\epsilon_{norm}}} \quad (1)$$

where α is the crossing angle, β^* the beta function at the interaction point and ϵ_{norm} is the normalized emittance at the IP. This approximation is valid only for the case where the β^* is much smaller than the s location of the first long-range encounter (for a 25 ns beam spacing this corresponds to 3.75m from the IP). This is valid for the IP1 and IP5 where the HL-LHC aims operating at β^* of 80-10cm. The schematic of the beam-beam interactions is shown in Figure 1. Operating with a crossing angle reduces the overlapping region between the two bunches crossing each other at the IP, this will result in a reduction of the luminosity, which is given by the integral of the two bunches overlap. Large crossing angle means reduced luminosity.

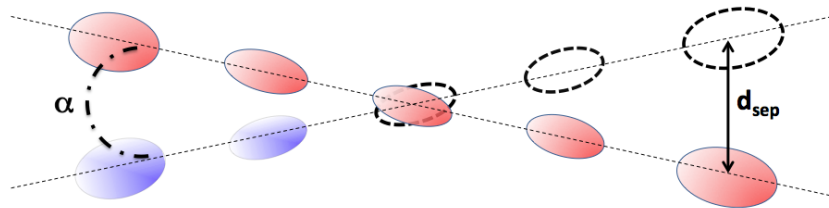


Fig. 1: Schematics of the beam-beam interactions geometry at an interaction point.

First estimates of the needed crossing angle to keep long range beam-beam effects weak fixed the external crossing angle α to 590 μrad for a β^* of 15 cm . This will give a beam-beam separation at the first encounter of 12.5σ . The real separations at the LR encounters are shown in Figure 2 and in Figure 3 for the ATLAS and the CMS interaction regions, respectively.

The corresponding footprint and Frequency Map Analysis (FMA) [15] is shown in Figure4. One can notice the zero amplitude particle shifted by roughly $\Delta Q_{x,y} = 0.007$. This corresponds approximately to $2 \cdot \xi_{bb}$ at the non-integer tunes of (0.31,0.32), where the beam-beam parameter ξ_{bb} is equal to 0.0035 per IP. This value is very similar to the LHC case [8]. Despite the very high brightness beams the effect

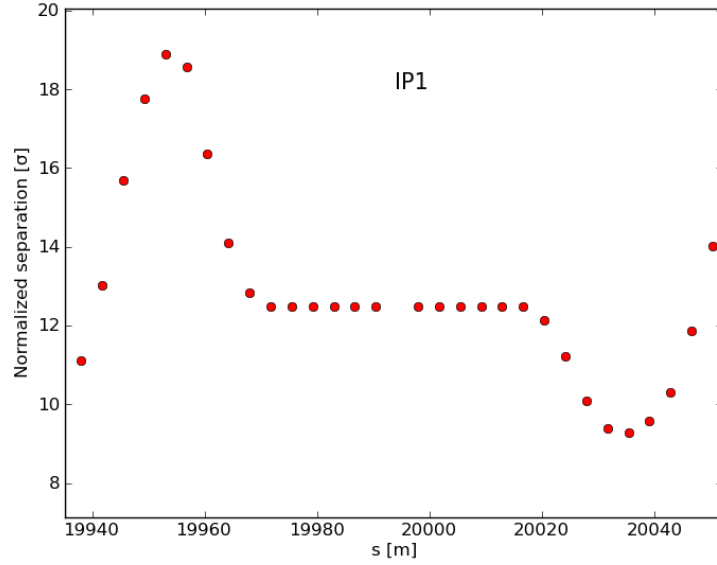


Fig. 2: Beam-beam long-range radial separation at the first 15 encounters left and right of the IP1 experiment. The separation in units of the beam RMS size at the IP, calculated for an emittance of $2.5 \mu\text{m}$ are shown as a function of the s location along the ring starting from IP3 in the HL-LHC sequence. The range shows the ATLAS interaction region.

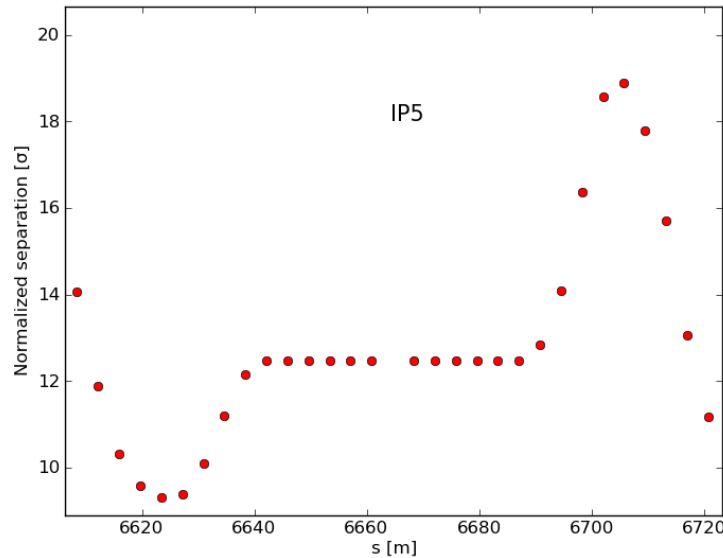


Fig. 3: Beam-beam long-range radial separation at the first 15 encounters left and right of the IP5 experiment. The separation in units of the beam RMS size at the IP, calculated for an emittance of $2.5 \mu\text{m}$ are shown as a function of the s location along the ring starting from IP3 in the HL-LHC sequence. The range shows the CMS interaction region.

of the head-on collision is very small due to the very large crossing angle. The beam-beam head-on tune shift is reduced in the presence of a crossing angle by the same factor which applies to the luminosity.

1.2 Crab crossing

As previously mentioned the HL-LHC relies on the use of crab cavities to compensate the geometric reduction factor coming from the finite crossing angle. The geometrical reduction factor due to the

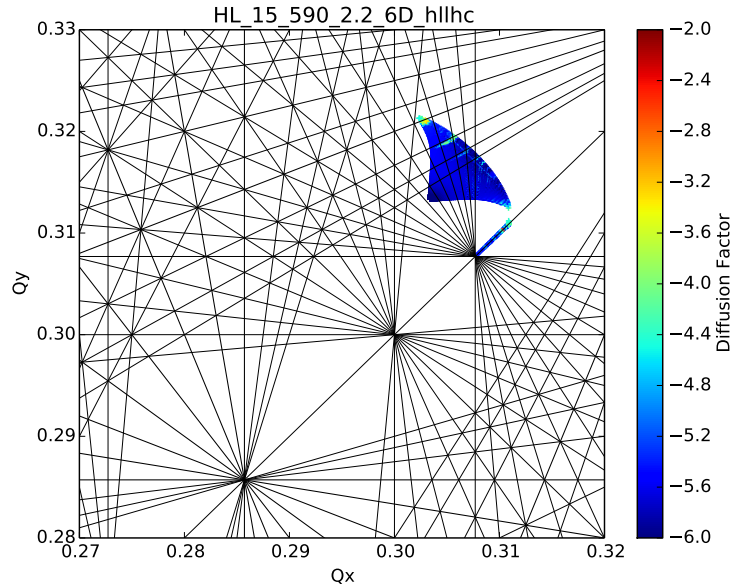


Fig. 4: Frequency Map Analysis of particles up to 6σ amplitude undergoing beam-beam head-on and long-range interactions in the two main IPs 1 and IP5 with a finite crossing angle α of $590\mu rad$.

crossing angle is estimated for the HL-LHC to be between 0.3-0.23%, depending on the bunch length of 7.5-10 cm. The use of crab cavities to compensate such a loss is explained in details in [4]. To allow for this new feature a modification of the numerical tools used for beam-beam studies was needed. Details of the code modifications can be found in Appendix B.

Crabbing the beams will have an impact on the head-on beam-beam interactions, while will leave un-perturbed the long-range interactions. The head-on beam-beam interaction will be larger respect to the case with a finite crossing angle of $590\mu rad$. This is visible in Fig. 5 that shows the modification to the tune footprint when a full crab crossing is applied at the IP1 and at the IP5. One can notice that as expected the zero amplitude particle is now shifted to a smaller frequency which corresponds to (0.287,0.297) which is roughly given by $\Delta Q_{x,y} = 2 \cdot \xi_{bb}$, where the beam-beam parameter ξ_{bb} is now equal to 0.011 per IP.

Comparing the FMAs corresponding to the two cases with and without crab-crossing one can notice from the diffusion factor that for the first case the long ranges seems exciting resonances involving tail particles (yellow dots on the footprint of Fig. 4) while in the case of a full head-on collision the core particles, pushed to lower frequencies parallel to the diagonal $Q_x = Q_y$, seem more involved and an increased diffusion indexes is visible (yellow dots in the footprint of Fig. 5). This just to highlight that the two cases are very different from the beam dynamics and need detailed study of possible mechanism that can deteriorate the beam parameters due to the very large head-on spread.

1.3 Crossing angle scan

A first study of the dependency of the dynamical aperture versus the crossing angles is shown in Figure 6 for the nominal beam parameters of the HL-LHC: $2.2 \cdot 10^{11}$ ppb and $\epsilon_{norm} = 2.5 \mu m$ for the HL-LHC optics with $\beta^* = 15$ cm. The configuration assumes beam-beam interactions head-on and long range in the two main IP1 and IP5. This linear dependence came from the fact that the strength of the BB interaction is proportional to the BB long range separation, that is proportional to crossing angle itself as shown in Eq. 1. The long-range separations in IP1 and IP5 are shown in Fig. 2 and Fig. 3, respectively. One can notice a reduction of the dynamical aperture of roughly 0.5σ at the nominal crossing angle of $590 \mu rad$. An impact of 0.5σ on the DA is in within error bars due to intensity and emittance fluctuations. Larger effects to maximum 1σ can be observed for smaller angles pointing to a possible enhancement of resonances driven by the long-range interaction in the presence of a much larger head-on contribution. The effect at smaller angles should be further studied. A linear dependency of the DA as a function of

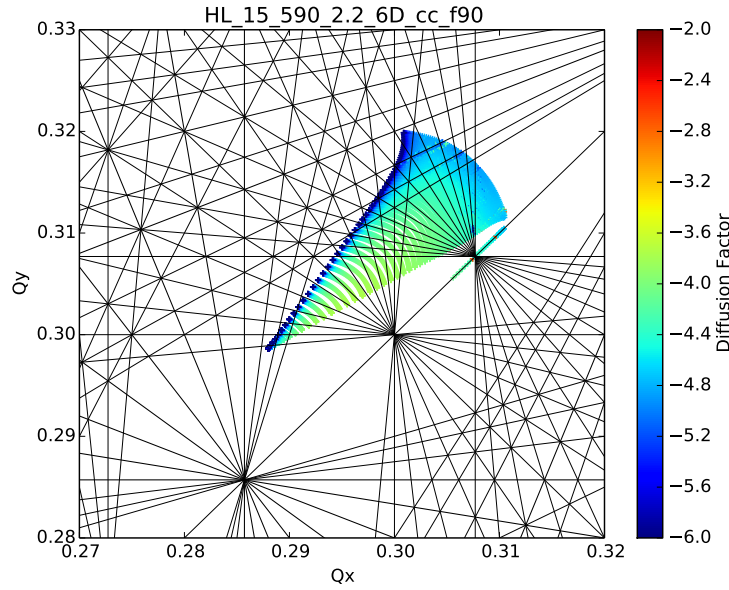


Fig. 5: Frequency Map Analysis of particles up to 6σ amplitude undergoing beam-beam head-on and long-range interactions in the two main IPs 1 and IP5. The head-on collisions experience a full crab crossing (zero crossing angle) while the long-range interactions are separated by an external crossing angle α of $590\mu rad$.

the crossing angle can be assumed for the HL-LHC case up to a crossing angle of $800\mu rad$ confirming the crossing angle scaling laws of DA found for the LHC [8].

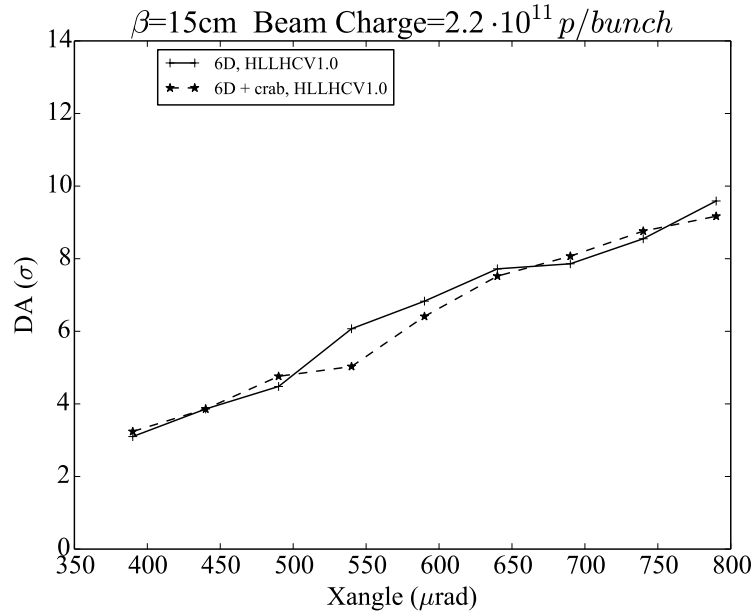


Fig. 6: Minimum DA for a crossing angle scan, beam charge of $2.2 \cdot 10^{11}$ and $\beta^* = 0.15$ m. Results with and without crab crossing are shown.

In Figure 7 we show the FMA in tune space (left plot) and in amplitude coordinates A_x and A_y which are expressed in units of the RMS beam size (right plot) for the nominal crossing angle of $590\mu rad$. The corresponding DA is as shown in Figure 6 to be around 6.4σ , nevertheless one can notice from the FMA of Figure 7 that several resonances have been excited and affect strongly particles down to 4.5σ . The diffusion factor is very large in the vicinity of the 13^{th} order resonance mainly perturbing the dynamics of large amplitude particles in the horizontal plane. In the Vertical plane particles

at larger amplitudes (7σ) are more sensitive to the 7^{th} and 5^{th} . Using the FMA one can identify the resonances which are excited and that are driving the dynamical aperture, in this case the 13^{th} order as also shown in [16]. Moreover it is visible from the FMA that when the system has a dynamic aperture of 6.3σ , actually particles from 4.8σ already show a perturbed behaviour which could be related to an earlier indicator of particle loss, has defined in [17].

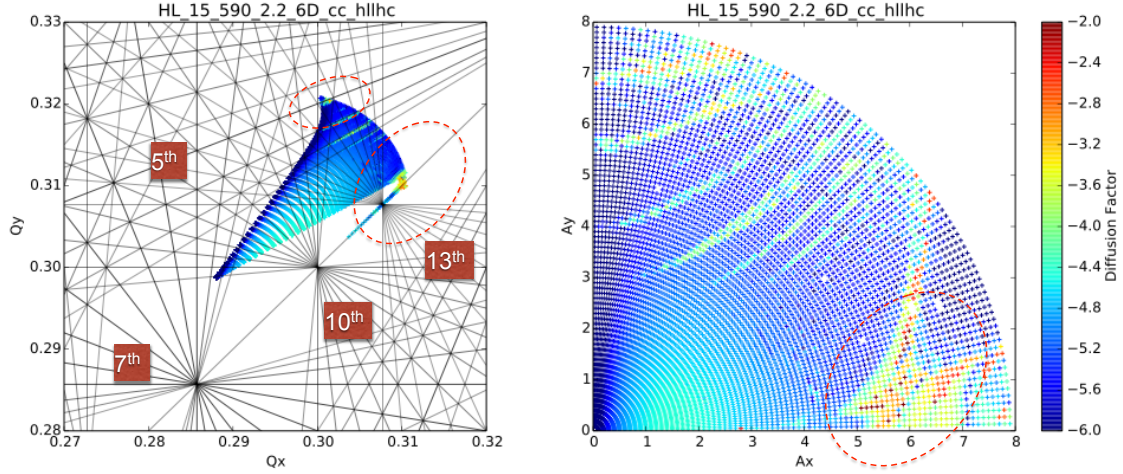


Fig. 7: FMA for the nominal configuration with crossing angle $\alpha=590\ \mu\text{rad}$, intensity $I_b=2.2\cdot 10^{11}\text{p/bunch}$, $\beta^*=0.15\text{ m}$ and full crab crossing. Left plot shows the FMA for particles up to 6σ amplitude in tune space while right plot is a FMA for particles up to 8σ amplitude

For comparison we show a case with larger crossing angle Figure 8 where the 7^{th} order resonance disappears and the 13^{th} order is much weaker. In this case the DA is identified at 8σ . If the angle is reduced to $490\ \mu\text{rad}$ the long-range interactions are stronger and particles at $4-5\sigma$ amplitude are lost. From the FMA of Figure 9 one can highlight that particles at 4σ are strongly affected by the 13^{th} order resonance. A big effort has been done to benchmark versus another model used for the Tevatron collider and results of some comparisons can be found in [13] and finally in the [4].

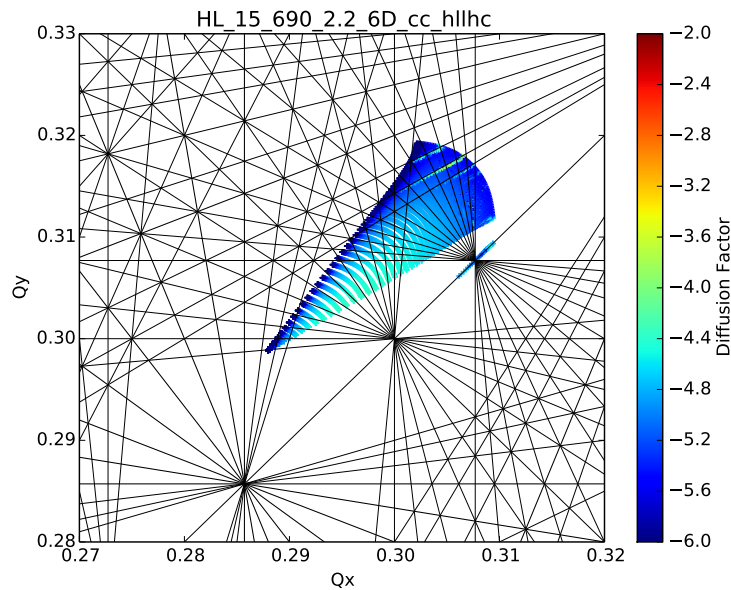


Fig. 8: FMA for particles up to 6σ amplitude for the nominal configuration with crossing angle $\alpha=690\ \mu\text{rad}$, intensity $I_b=2.2\cdot 10^{11}\text{p/bunch}$, $\beta^*=0.15\text{ m}$ and full crab crossing.

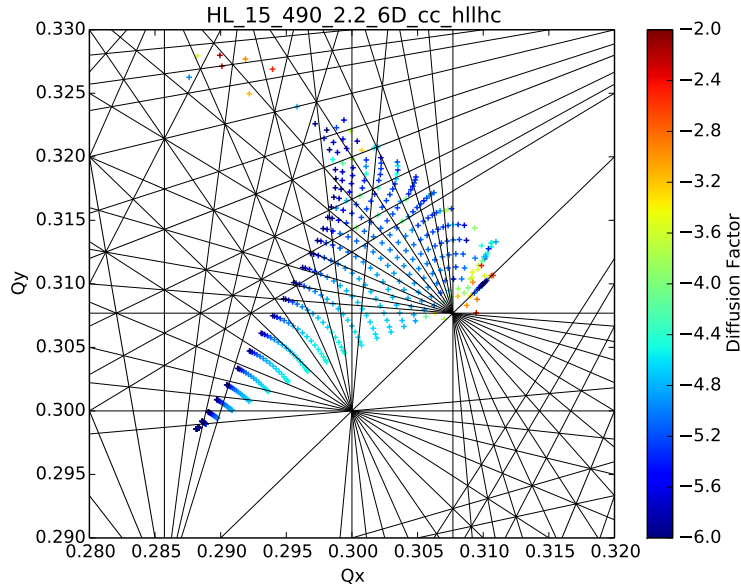


Fig. 9: FMA for $\alpha=490 \mu\text{rad}$ crossing angle, $I_b=2.2 \cdot 10^{11} \text{p/bunch}$ and $\beta^*=0.15 \text{ m}$

1.4 Intensity scan

In Figure 10 the dependence of DA on the bunch population is shown, for $\alpha=590 \mu\text{rad}$. The DA is always larger than 6σ for the nominal crossing angle configuration and in the range of interest between 1 and $2.2 \cdot 10^{11}$ protons per bunch. The linear scaling law of DA versus intensity is confirmed also for the HL-LHC baseline crossing angle and minimum β^* .

A different behavior is shown between crabbed and un-crabbed case for intensities in the range of 2.2 and $3.0 \cdot 10^{11} \text{ p/bunch}$ where a difference up to 1σ DA is observed. For the case with crab-crossing the DA degrades faster. If we analyze the FMAs for different intensities in Figure 11, 12 and 13 we can notice that for higher intensities the FMA shows a much larger diffusive mechanism on top of the 13^{th} order resonance.

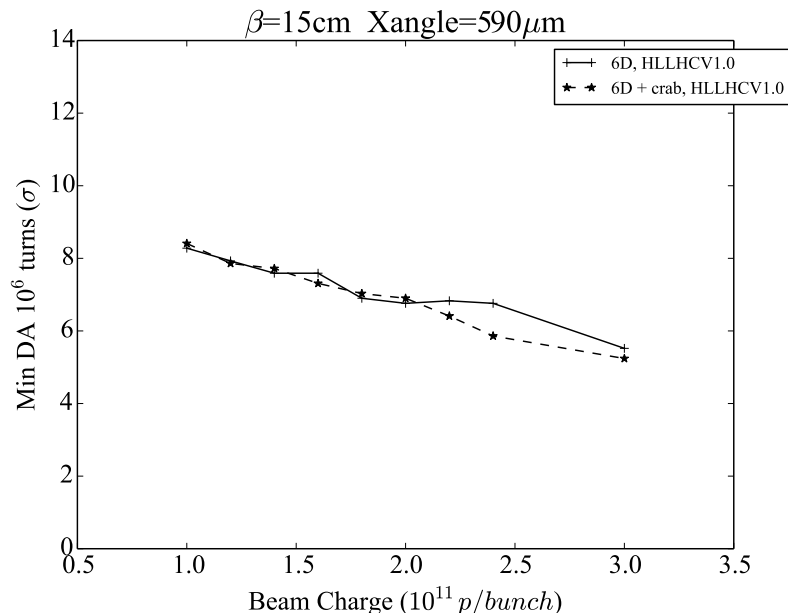


Fig. 10: Minimum DA for a beam intensity scan, $\alpha=590 \mu\text{rad}$ and $\beta^*=0.15 \text{ m}$. Result with and without crab crossing are shown.

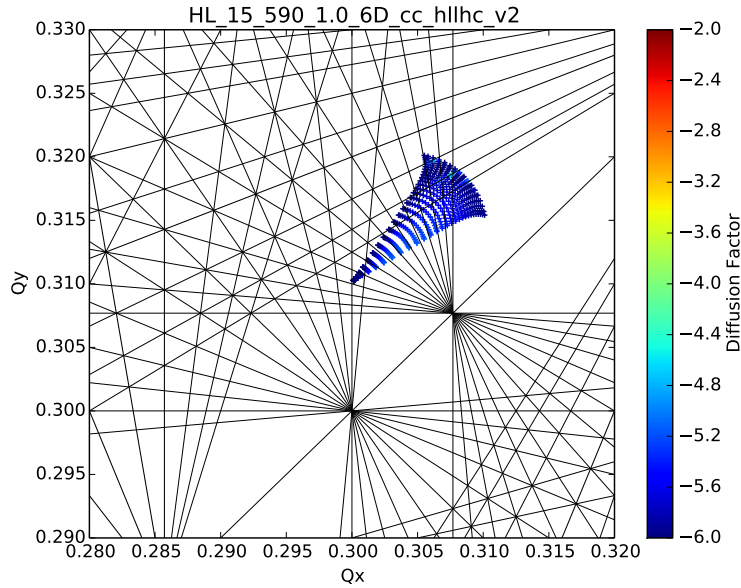


Fig. 11: FMA for an intensity $I_b=1.0 \cdot 10^{11}$ p/bunch, $\alpha=590 \mu\text{rad}$ and $\beta^*=0.15$ m.

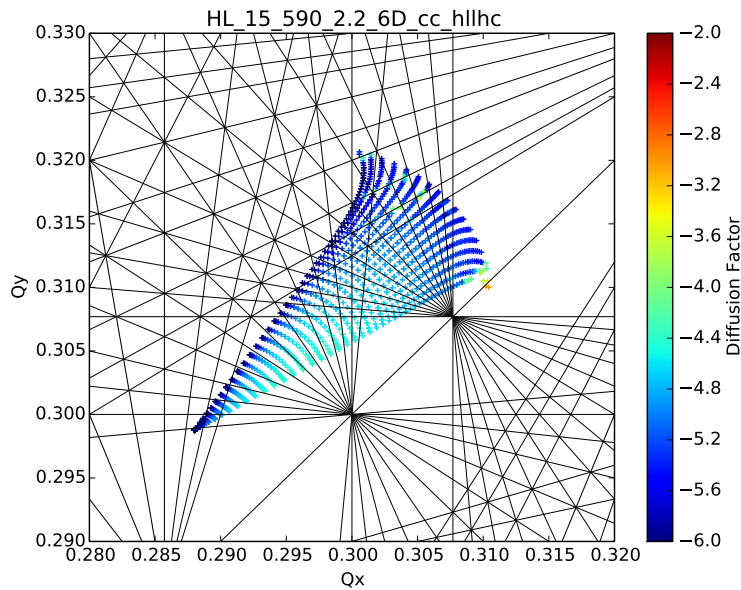


Fig. 12: FMA for an intensity $I_b=2.2 \cdot 10^{11}$ p/bunch, $\alpha=590 \mu\text{rad}$ and $\beta^*=0.15$ m.

1.5 Errors

A campaign to evaluate the effect of magnetic field errors on the beam dynamics in the presence of beam-beam interactions has also been performed at top energy. Multipolar errors have been set-up following specifications in [18]. Typically 60 different sets (seeds) of the field errors are used for each case. Results are in Fig. 14, where the minimum, maximum and average DA are also shown for the nominal case, with full crab crossing. As visible, including multipolar error introduce a modification of the beam dynamics, a maximum deviation of less than 0.5σ is expected for the nominal crossing angle of $590 \mu\text{rad}$. The contribution at larger crossing angles is more important, up to 2σ reduction. This behaviour is consistent with the fact that when long-range beam-beam are weak the DA is dominated by the machine non-linearities (i.e. multipolar errors). As also observed in LHC data [11]. Moreover the criteria of using the minimum DA is the most conservative and we choose this parameter for deciding on the optimum set of parameters for best beam lifetimes.

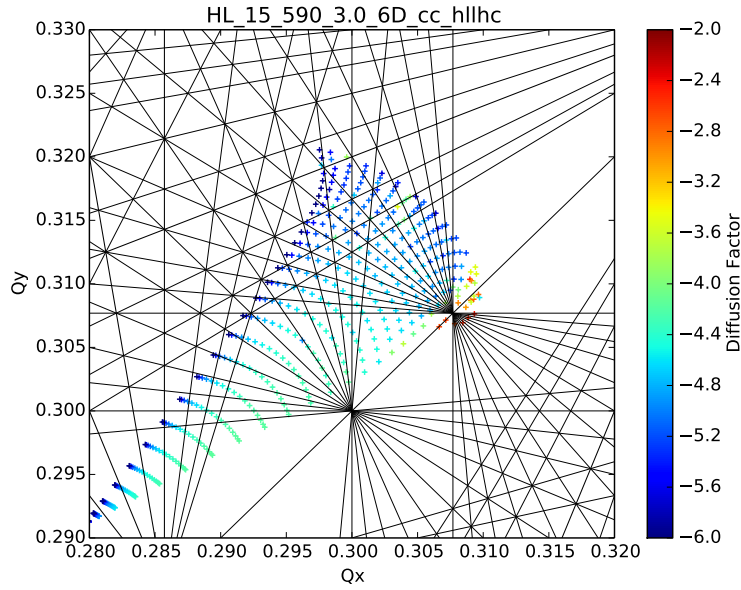


Fig. 13: FMA for an intensity $I_b=3.0 \cdot 10^{11}$ p/bunch, $\alpha=590 \mu\text{rad}$ and $\beta^*=0.15$ m.

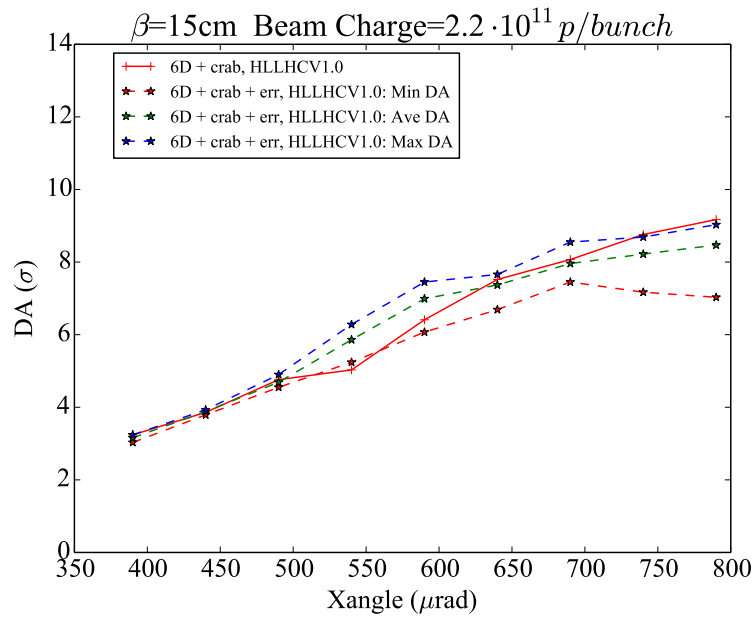


Fig. 14: Dynamic Aperture as a function of the crossing angle due to beam-beam effects (red solid line), minimum DA (red dashed line), average DA (green dashed line) and maximum DA (blue dashed line) for a nominal beam configuration.

In Figure 15 we show the contribution of the multipolar errors with and without the use of crab cavities. At the nominal crossing angle of $590 \mu\text{rad}$ a reduction of maximum 0.6σ should be expected for the nominal beam case. For the HL-LHC scenario the multipolar errors have a very small impact. What dominates the dynamics are the long-range beam-beam interactions. A 10% deviation in intensity or in crossing angle will have a much larger impact than the multipolar errors. However at larger angle the non-linearities from the magnets become dominant and no improvement is observed. This shows that the crossing angle of $590 \mu\text{rad}$ is the largest acceptable, above it the dynamics is dictated by the non-linear errors.

In Fig. 16 and 17 we show the minimum DA as a function of the XY plane angle of the simulated particles for an intensity of $1.1 \cdot 10^{11}$ and $2.2 \cdot 10^{11}$ protons per bunch. All the 60 seeds used for the

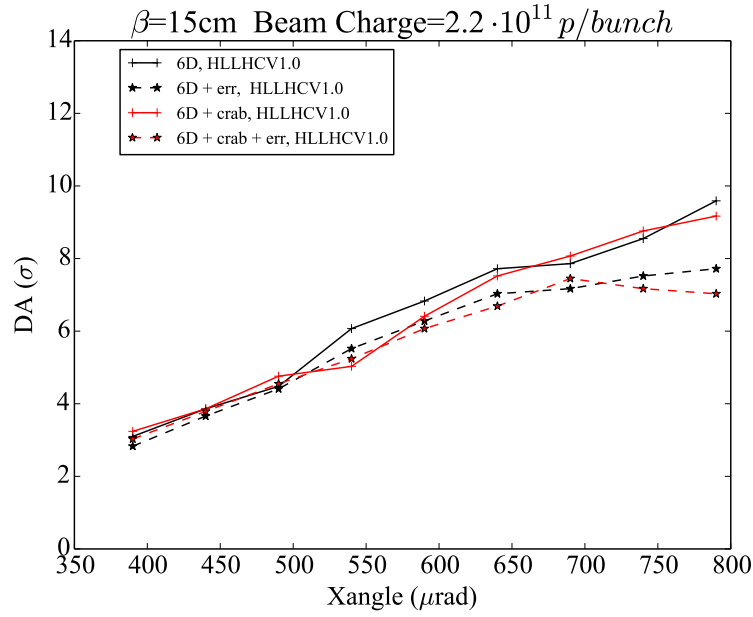


Fig. 15: Minima DA as a function of the crossing angles in IP1 and IP5. Result with (red lines) and without (black lines) crab crossing are shown. Dashed lines correspond to the case with multipolar errors.

multipolar error are shown, for the nominal case at two bunch population. The average and minimum DA are shown respectively in green and red. The minimum DA is always within 3σ of standard deviation among the 60 seeds results, for this reason we can state that quoting the minimum DA is a conservative but still representative way to evaluate the impact of the multipolar errors distributions in the accelerator.

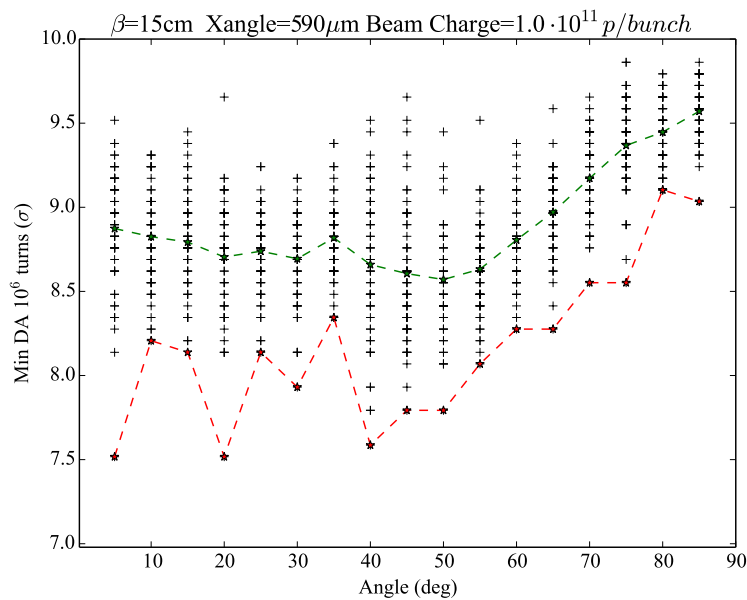


Fig. 16: Dynamic Aperture as a function of the particle XY angle. All 60 seeds used are shown, black crosses, with the minimum (red dashed line) and average (green line) DA highlighted for $I_b = 1.0 \cdot 10^{11} p/bunch$

One can notice in Figure 16 that the impact of the multipolar errors is much stronger respect to the case at higher intensities. For this case the multipolar errors will reduce the DA by 1σ . This points to the fact that when beam-beam interactions are weaker the DA is mainly dominated by the accelerator non-linearities. While when the beam-beam interactions are strong, as visible in Figure 15 at angles

below and equal to $590 \mu rad$, the multipolar errors do not impact the dynamics.

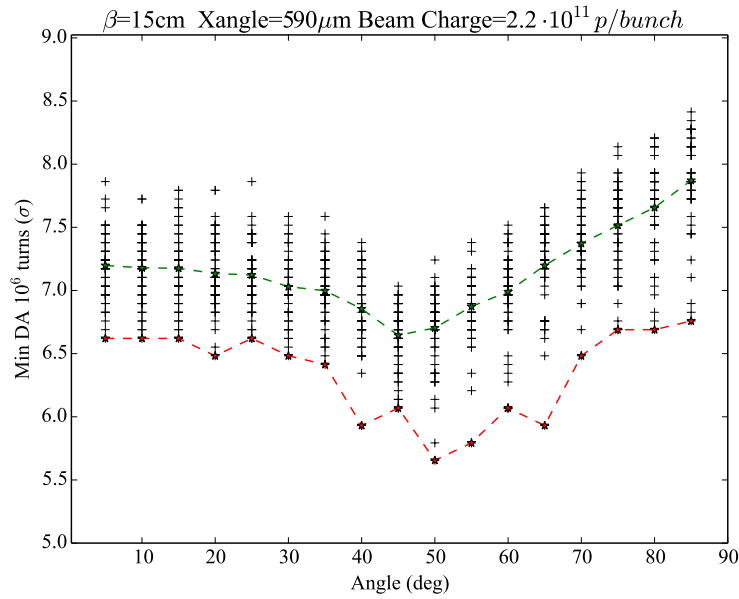


Fig. 17: Dynamic Aperture as a function of the particle XY angle. All 60 seeds used are shown, black crosses, with the minimum (red dashed line) and average (green line) highlighted for $I_b = 2.2 \cdot 10^{11}$ p/bunch

Another important information we wanted to identify are the contributions from the various elements in the interaction region. We have simulated the dynamical aperture turning on and off the various elements and compare to the general cases without and with full multipolar errors set. In Figures 18 and 19 we show the results for two bunch populations. The multipolar errors are applied separately to each magnet element. As visible the multipolar errors of the Inner Triplets (IT) are the one dominating and causing most of the DA degradation. To improve the dynamic aperture of the HL-LHC it is important to optimize the multipolar errors of these elements and keep enough margins.

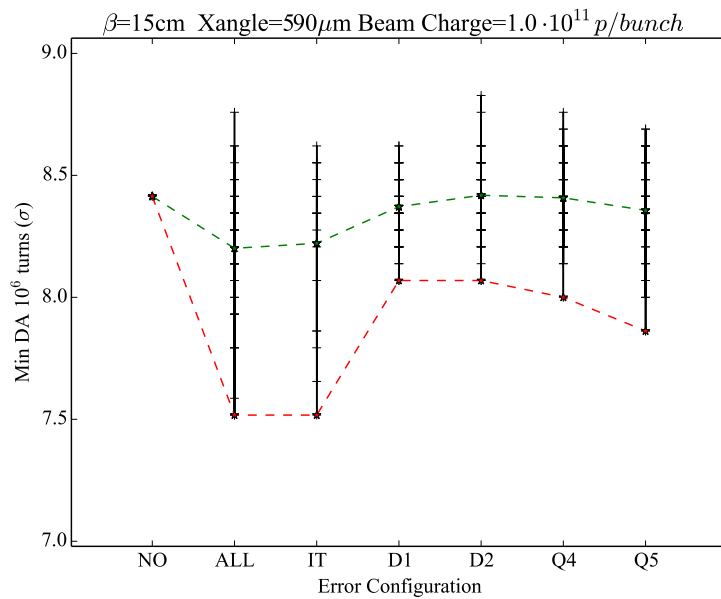


Fig. 18: Effect of multipolar error sorted by magnet element. Minimum (red) and average (green) DA for 60 seeds are shown. $I_b = 1.0 \cdot 10^{11}$ p/bunch

For the HL-LHC case at β^* of 15 cm and intensity of $2.2 \cdot 10^{11}$ protons per bunch and a crossing angle of $590 \mu rad$ we expect a DA of 5.6σ which is not acceptable. Moreover we still need to identify the

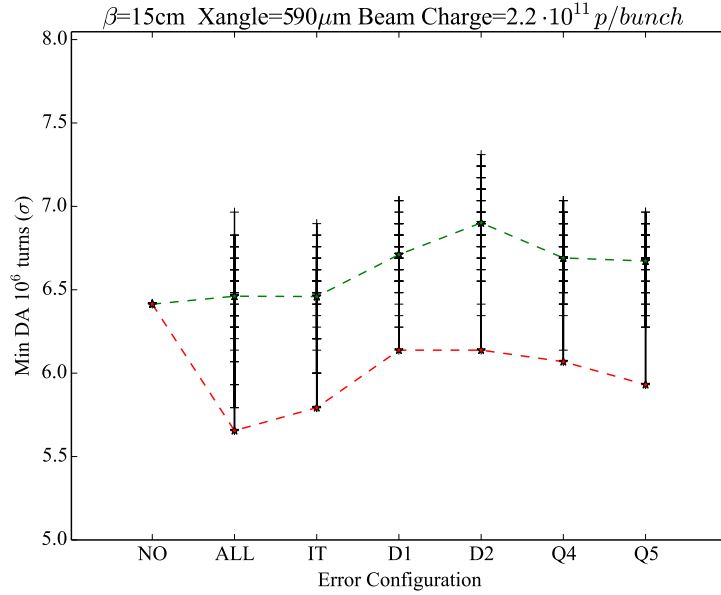


Fig. 19: Effect of multipolar error sorted by magnet element. Minimum (red) and average (green) DA for 60 seeds are shown. $I_b = 2.2 \cdot 10^{11}$ p/bunch

contribution from two larger β^* experiments IP2 and IP8. More details on the field quality requirements in the presence of beam-beam interactions can be found in [19] where many of the results described in these note have been presented.

1.6 β^* leveling

The peak luminosity that the HL-LHC operational baseline can provide is too challenging for the physics experiments: the need to level the luminosity to a lower value to guarantee the optimum conditions to the detectors to resolve the physics events is crucial. Various techniques are available (e.g. transverse offset, larger β^*) and they have an important impact on the beam-beam dynamics as shown in [20]. For the HL-LHC the baseline scenario foresees the use of leveling with the β^* since this ensures larger margins from the beam-beam dynamics, as one can intuitively deduce from Eq. 1. With this technique we will show that one can fulfill the criterion of a minimum DA larger than 6σ with further margins for higher intensities and/or reduced crossing angle operation. A minimum 6σ DA cannot be guaranteed otherwise [21].

In Table 2 the main parameters for the baseline case are shown. In Fig. 20 the minimum DA as a function of the crossing angle scan is shown for four different β^* values simulating a possible operational scenario.

L	I_b at $\beta^*=40\text{cm}$	I_b at $\beta^*=33\text{cm}$	I_b at $\beta^*=15\text{cm}$	I_b at $\beta^*=10\text{cm}$
($10^{34}\text{cm}^{-2}\text{sec}^{-1}$)	10^{11} (p/bunch)	10^{11} (p/bunch)	10^{11} (p/bunch)	10^{11} (p/bunch)
5	1.7	1.5	1.1	1
7.5	–	2.1	1.5	–

Table 2: Bunch population during β^* leveling for the baseline and ultimate scenarios.

In Figures 20, 21, 22 and 23 we plot the minimum DA as a function of the crossing angle for several intensities. With these studies we can identify the maximum bunch population acceptable per optics (β^*) as a function of the crossing angle.

In Figure 24 the minimum DA during a β^* leveling is shown for two different values of leveled

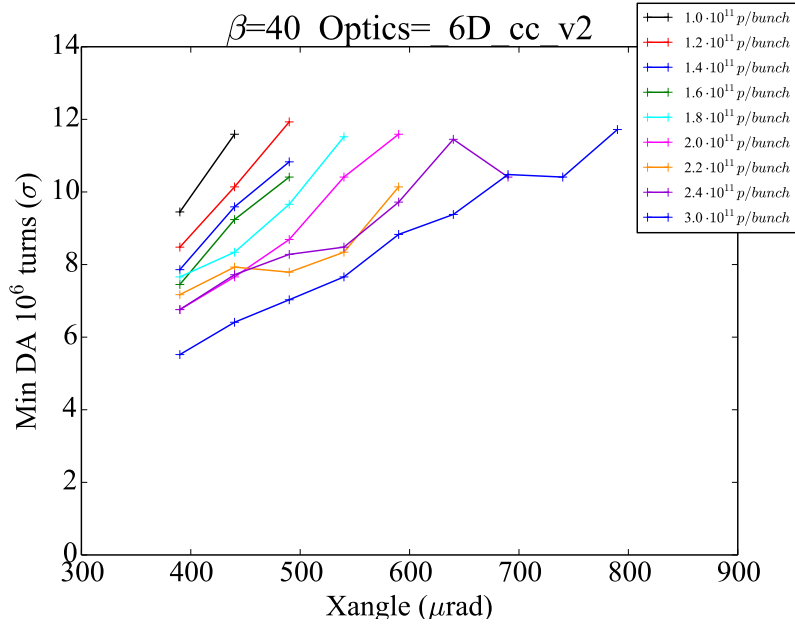


Fig. 20: Minimum DA as a function for the crossing angles in IP1 and IP5 for different bunch populations. All cases are for a $\beta^*=40$ cm.

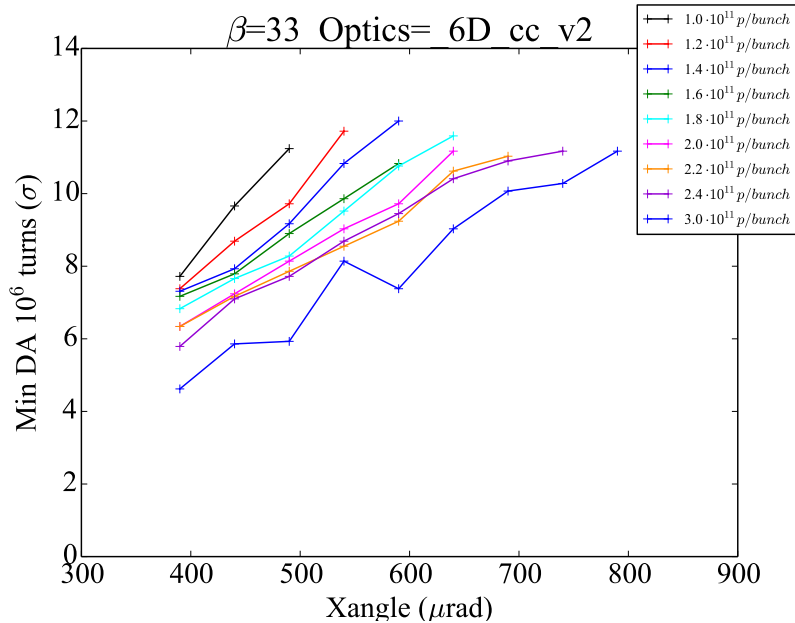


Fig. 21: Minimum DA as a function for the crossing angles in IP1 and IP5 for different bunch populations. All cases are for a $\beta^*=33$ cm

luminosity. As visible the β^* leveling scenario at nominal crossing angle of 590μ rad is robust and provide a minimum DA that is always above the 6σ for both leveled luminosity of $5 \cdot 10^{34} \text{cm}^{-2} \text{s}^{-1}$ (black lines) and $7.5 \cdot 10^{34} \text{cm}^{-2} \text{s}^{-1}$ (red lines). Thanks to the β^* leveling techniques the beam-beam long range interactions are much weaker than in a fully squeezed optics as one can deduce from Eq. 1 and this gives room to a reduction of the crossing angle down to 450μ rad for β^* larger than 15 cm as shown in Figure 24 blue lines. The margins acquired with the use of the β^* leveling technique can be also used to increase the bunch population by almost a factor 2, respect to the assumed value of Table2, as visible on the intensity scans of Figures ???. This intensities goes beyond the HL-LHC project parameter space but shows the potentialities of the HL-LHC upgrade coming from the beauty of the beta* leveling technique to reduce beam-beam effects.

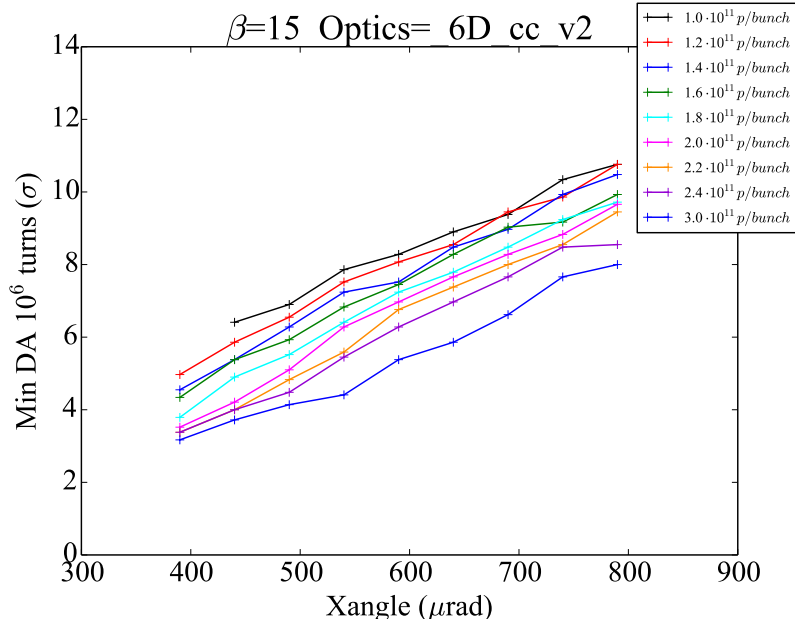


Fig. 22: Minimum DA as a function for the crossing angles in IP1 and IP5 for different bunch populations. All cases are for a $\beta^*=15$

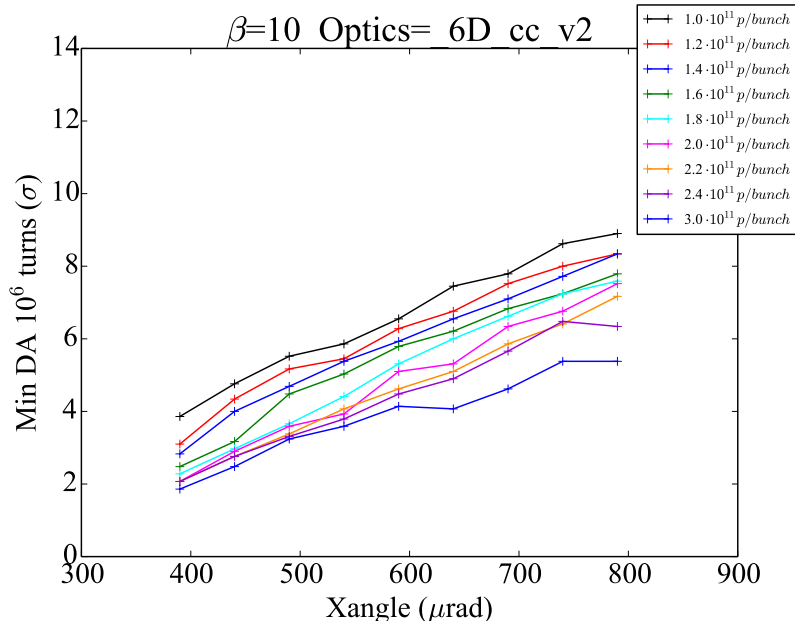


Fig. 23: Minimum DA as a function for the crossing angles in IP1 and IP5 for different bunch populations. All cases are for a $\beta^*=10$.

Alternative scenarios have also been evaluated with DA studies and have been proposed and presented in [22]. Where the study of a possible flat-optics together with the β^* leveling techniques have shown important alternatives to the use of crab cavities in case of issues in the operation of these devices. This proposal is used as a back-up solution for the HL-LHC project.

1.7 IP8 and IP2 impact and settings

In all the simulation shown before only IP1 and IP5 were considered, while IP2 and IP8 were not colliding and fully separated. As a design strategy we wanted to set and optimize the HL-LHC scenarios with the two main high luminosity experiments, IP1 and IP5, driving the beam-beam dynamics. The other experiments, IP8 and IP2, should be set in the shadow of these two main experiments. We evaluated the

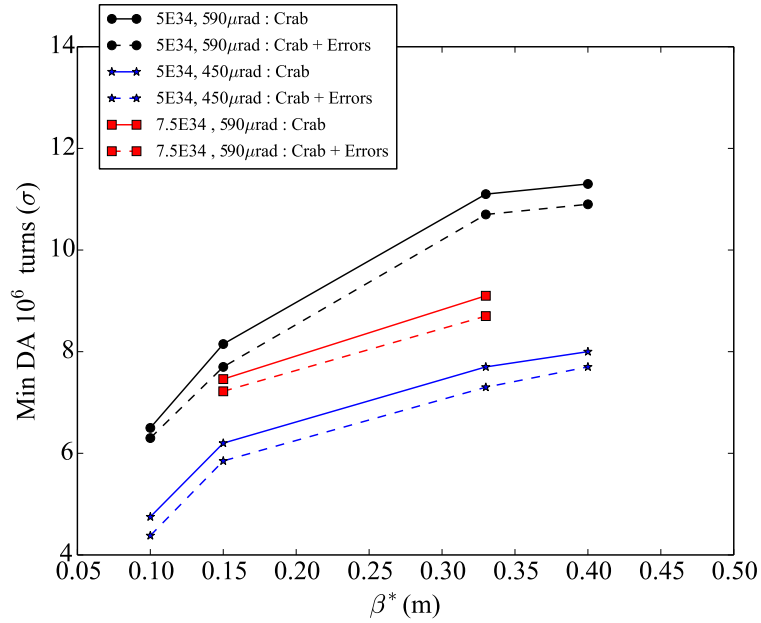


Fig. 24: Minimum DA as a function of the β^* with (dashed lines) and without (solid lines) multipolar errors. Two leveled luminosity scenarios are shown: the baseline $L=5\cdot 10^{34}\text{cm}^{-2}\text{sec}^{-1}$ (black lines) and the ultimate $L=7.5\cdot 10^{34}\text{cm}^{-2}\text{sec}^{-1}$ (red lines). An alternative scenario with reduced crossing angle of $450\ \mu\text{rad}$ (red lines) is also shown.

contribution of the LHCb experiment and suggest also a leveling technique to reduce to the minimum its impact.

In Figure 25 and Fig. 26 the effect of additional collision in IP8 is shown, for the nominal case: full crab crossing in IP1 and IP5 while a finite crossing angle is applied at IP8 (external half angle $250\ \mu\text{rad}$, spectrometer in and $\beta^* = 3\ \text{m}$).

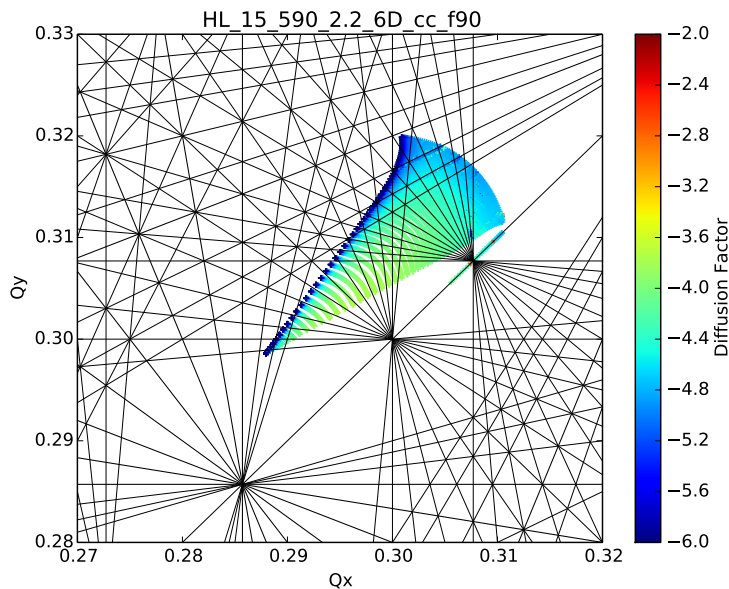


Fig. 25: FMA for the nominal case with intensity $I_b=2.2\cdot 10^{11}\text{p/bunch}$, $\alpha=590\ \mu\text{rad}$ at IP1 and IP5 and $\beta^*=0.15\ \text{m}$. No collision from IP8.

The crossing scheme in IP8 consists in the combination between an external crossing angle that can be varied and the angle given by the LHCb spectrometer that at top energy corresponds to an extra

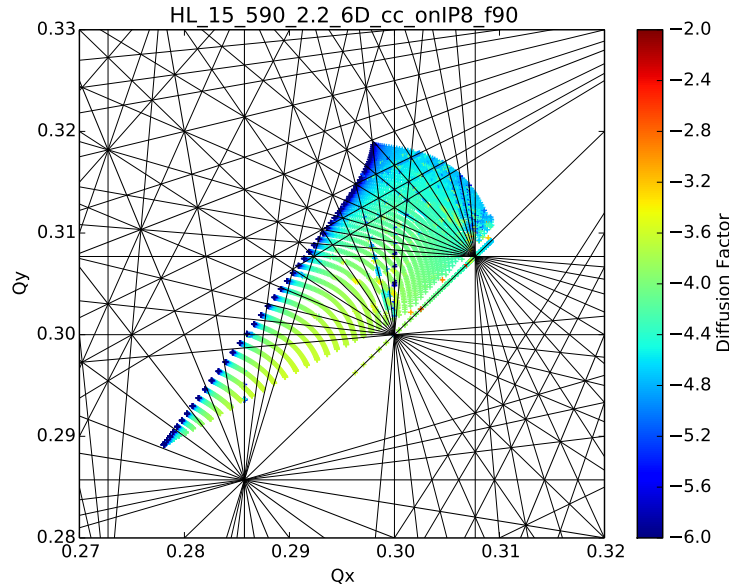


Fig. 26: FMA for the nominal case with intensity $I_b=2.2 \cdot 10^{11}$ p/bunch, $\alpha=590 \mu\text{rad}$ at IP1 and IP5 and $\beta^*=0.15$ m. With full collision in IP8 with external crossing angle of .

angle of $270 \mu\text{rad}$ which could add or subtract to the external crossing depending on chosen polarity, details of the scheme could be found in [23]. In Tab. 3 the DA computed for different external crossing angles and spectrometer polarities are listed to show the maximum deviation on the DA. When the spectrometer polarity is set to positive the impact of the IP8 to the DA is a reduction of $0.5\text{-}0.7 \sigma$ for external crossing angles of 560 and $340 \mu\text{rad}$ as visible in Table 3. If the polarity is negative then a test for an external crossing angle of $340 \mu\text{rad}$ shows an impact of 0.3σ on the DA. The impact is smaller at smaller intensities, as expected.

I_b	IP8 off	IP8	IP8	IP8
		ext = $-340 \mu\text{rad}$ spec = $-270 \mu\text{rad}$	ext = $-560 \mu\text{rad}$ spec = $+270 \mu\text{rad}$	ext = $-340 \mu\text{rad}$ spec = $+270 \mu\text{rad}$
1.0	8.41	8.07	7.93	7.72
2.2	6.42	6.28	6.06	5.86

Table 3: IP8 effect for different collision configurations

The HLLHC baseline is based on leveling the luminosity in the IP2 and IP8 by separation to reduce the impact on DA and on other effects as noise on colliding beams which are directly related to the overall tune spread induced by beam-beam interactions. In Figure 27 we show the DA as a function of the crossing angle in IP1 and IP5 for the baseline configuration where collisions at $15 \text{ cm}\beta^*$ are foreseen at an intensity of $1 \cdot 10^{11}$ p/bunch. The case with only IP1 and IP5 versus different configurations of IP2 and IP8 are plotted. For this intensity the impact on the dynamic aperture is marginal even if all four experiments collide head-on (IP1 and IP5 with crab crossing while IP2 and IP8 in their baseline configuration as specified in [3]). Different transverse separation have been evaluated and the impact of the beam-beam effects arising from IP2 and IP8 on the dynamic aperture shows to be less than 1σ at the nominal crossing angle of $590 \mu\text{rad}$. For this case a possibility to reduce the operational crossing angle to $450 \mu\text{rad}$ is not out of range with some further optimization.

In case that the luminosity cannot be leveled by β^* then the impact of beam-beam effects from IP2 and IP8 is much stronger and a 6σ dynamic aperture is not guaranteed at the nominal crossing angle of $590 \mu\text{rad}$. A scenario with head-on collisions with finite external crossing angles of $340 \mu\text{rad}$ for IP2 and of $500 \mu\text{rad}$ for IP8 will corresponds to a DA of 4σ , which has been proved experimentally to lead

to very bad lifetimes [12].

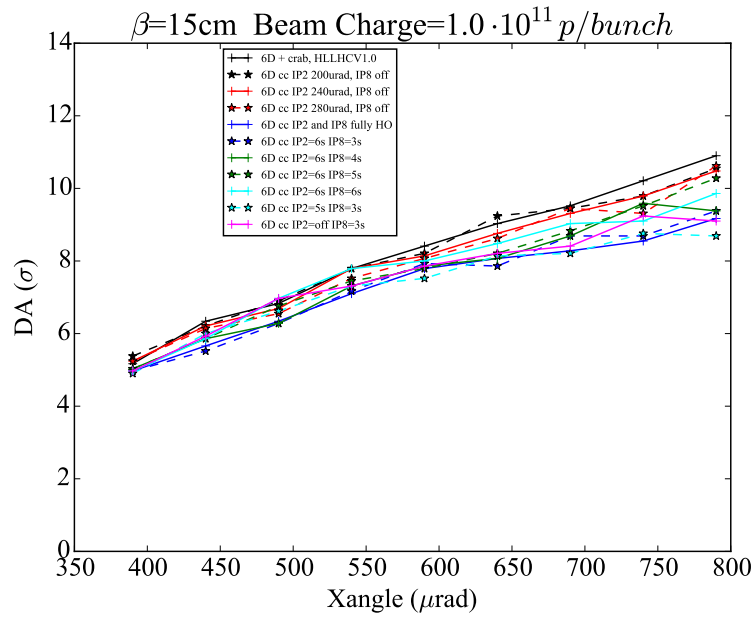


Fig. 27: DA as a function of the crossing angle in IP1 and IP5 for different configurations of the IP2 and IP8 crossing schemes. We compare the impact of leveling the IP2 and IP8 with a transverse offset at different amplitudes and for different effective crossing angles of IP2 for the case with a bunch intensity of $1.0 \cdot 10^{11}$ p/bunch. The IP8 half external crossing angle is set to $250 \mu rad$ and the spectrometer on positive polarity (subtracts to the external angle).

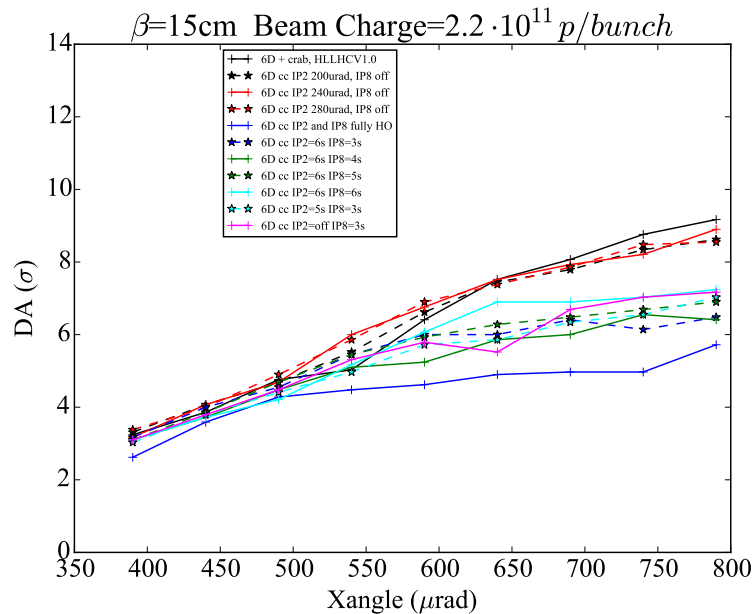


Fig. 28: DA as a function of the crossing angle in IP1 and IP5 for different configurations of the IP2 and IP8 crossing schemes. We compare the impact of leveling the IP2 and IP8 with a transverse offset at different amplitudes and for different crossing angles of IP2 for the case with a bunch intensity of $2.2 \cdot 10^{11}$ p/bunch. The IP8 half external crossing angle is set to $250 \mu rad$ and the spectrometer on positive polarity (subtracts to the external angle).

2 HL-LHC Weak-Strong Beam-Beam studies summary

In Figure 29 we plot the Dynamical Apertures evaluated for the different steps in β^* for the HLLHC Baseline and Ultimate scenarios as defined in [3]. The HLLHC Baseline is robust thanks to the choice of using the β^* leveling which makes the beam-beam long range interactions negligible. Comparing to the LHC, we can state that the long range impact to the dynamics will be much weaker than what was already been observed in the LHC during the 2012 and 2015 physics run. To keep larger margins we also propose to level the luminosity in the IP2 and IP8 by separation leveling to reduce the impact on DA as visible in Figure 27 and 28.

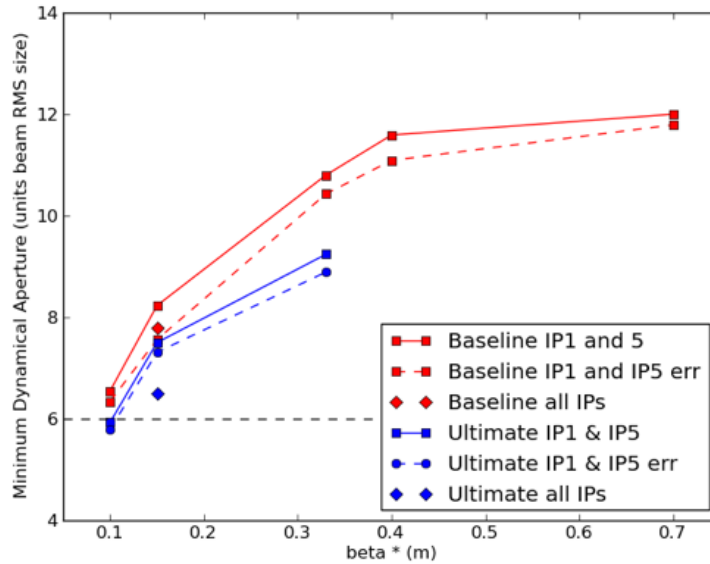


Fig. 29: Dynamical Aperture results summary for the HL-LHC Baseline (red markers) and Ultimate (blue markers) scenarios as described in [3]. The solid lines refer to the dynamical aperture due to beam-beam interactions head-on and long range at the main high luminosity experiments: IP1 and IP5 colliding at a finite crossing angle of $590 \mu rad$. Dashed lines refer to the estimated dynamical aperture when multipolar errors are added to the model of the machine lattice for both scenarios. Diamonds show the impact coming from the IP2 colliding with a transverse offset of 5σ for both cases and IP8 colliding with a transverse offset of 0σ (red diamond) and 3σ (blue diamond) for the Baseline and Ultimate scenarios, respectively. The IP8 half external crossing angle is set to $250 \mu rad$ and the spectrometer on positive polarity (subtracts to the external angle). The IP2 half external crossing angle is set to $170 \mu rad$.

Several studies on the impact of the machine chromaticity and octupoles have also been addressed and have been presented in [14, 24]. It has been found that a preferred polarity of the Landau Octupoles when a pick beta in the arcs of 1 Km is used can actually improve the DA in the presence of beam-beam. These preliminary studies show the possibility to actually compensate the reduction of Dynamical Aperture due to beam-beam by the use of octupole magnets in a global way. This finding is of course of interest for the HL-LHC project since it opens the possibility to work on a possible reduced crossing angle scheme for the alternative scenario as proposed in [22] in the case of problems with crab-cavities. The impact of chromaticity as also been evaluated in [14] and recommendation to operate a low chromaticity is proposed when the beams are colliding. In parallel to the round optics case detailed studies on a flat-optics have been carried and results have been compared to the round optics case in [25]. A possible scenario with flat optics have been proposed [22] and optimization is still possible to boost the luminosity performance of such a scheme [26].

3 Acknowledgements

A special thank to G. Arduini for the valuable comments and discussions on the work presented in this paper, E. Metral and A. Valishev for the constant support. All the simulations shown could have

been performed only thanks to the BOINC Project. We would like to take the chance to thank all the volunteers for supporting us and the project. A big thank is also deserved by the LHC@home Team at CERN, particularly by E.McIntosh, R. De Maria and I.Zacharov, and to the EPFL and the HL-LHC project for the financial support to the study.

4 References

- [1] "The High Luminosity Large Hadron Collider", Editors O. Bruning and L. Rossi, advanced Series on Directions in High Energy Physics-Vol. 24, World Scientific, 2015.
- [2] S. Fartoukh, "Achromatic telescopic squeezing scheme and application to the LHC and its luminosity upgrade", Phys. Rev. ST Accel. Beams 16, 111002, November 2013.
- [3] G. Arduini et al., "HL-LHC OPERATIONAL SCENARIOS", CERN-ACC-NOTE-2015-0009, May 2015.
- [4] The HiLumi LHC Collaboration, "HL-LHC PRELIMINARY DESIGN REPORT", CERN-ACC-2014-0300, Nov. 2014.
- [5] F. Schmidt, "Single Particle Tracking Code Treating Transverse Motion with Synchrotron Oscillations in a Symplectic Manner", CERN SL 94-56 (AP).
- [6] K. Hirata, H. Moshhammer and F. Ruggiero, "A symplectic beam-beam interaction with energy change", Particle Accelerators, 1993, Vol.40, pp.205-228.
- [7] M. Bassetti and G.A. Erskine, "Closed expression for the electrical field of a two-dimensional Gaussian charge", CERN, CERN-ISR-TH/80-06, (1980).
- [8] LHCDesign Report.
- [9] J. P. Koutchouk, for the LHC Team, "The LHC Dynamic Aperture", Proceedings of the 1999 Particle Accelerator Conference, New York, 1999.
- [10] R. Assmann et al., "Results of Long-range beam-beam studies-scaling with beam separation and intensity", CERN-ATS-Note-2012-070 MD, Geneva 2012.
- [11] M. Crouch et al., "DYNAMIC APERTURE STUDIES OF LONG-RANGE BEAM-BEAM INTERACTIONS AT THE LHC", 8th International Particle Accelerator Conference, 14-19 May, Copenhagen, Denmark, (2017).
- [12] T. Pieloni et al., "Beam-Beam Head-on and Long-Range Effects", EVIAN Operational Workshop 2015, EVIAN, France, 2015.
- [13] A. Valishev for WP2 Task 2.5 Joint "Beam-beam Studies for HL-LHC", Joint LARP CM20 HiLumi Meeting April 8-10, 2013.
- [14] J. Barranco and T. Pieloni, "Global compensation of long-range beam-beam effects using octupole magnets: dynamic aperture simulations for the HL-LHC case and possible usage in LHC and FCC.", CERN-ACC-NOTE-2017-XXX, 2017.
- [15] J.Laskar, "Frequency Map Analysis and Particle Accelerators", Proceedings of the 2003 Particle Accelerator Conference, 2003.
- [16] W. Herr and D. Kaltchev, "Effect of phase advance between interaction points in the LHC on the beam-beam interaction", LHC-PROJECT-Report-1082.
- [17] Y. Luo and F. Schmidt, "Dynamic Aperture Studies for LHC Optics Version 6.2 at Collision", LHC-PROJECT-Report-310.
- [18] M. Giovannozzi et al., "DYNAMIC APERTURE PERFORMANCE FOR DIFFERENT COLLISION OPTICS SCENARIOS FOR THE LHC LUMINOSITY UPGRADE", IPAC2013, Shanghai, China, 12-17 May, 2013.
- [19] T. Pieloni et al., "Field Quality Requirements including beam-beam effects", presentation at Joint HiLumi-LARP Meeting, 11-13 May 2015 Fermilab, USA.
- [20] X. Buffat et al., "Beam-beam Effects in Different Luminosity Levelling Scenarios for the LHC", Proceedings of IPAC2014, Dresden, Germany, 2014.
- [21] D. Banfi et al., "Weak-strong Beam-Beam Simulations for the HL-LHC", Proceeding of IPAC2014, Dresden, Germany, 2014.
- [22] R. Tomas et al., "HL-LHC Alternatives Scenarios", Proceedings of Chamonix 2014 Workshop on the LHC Performance, Chamonix, France, 2014.

- [23] W. Herr and Y. Papaphilippou, "Alternative running scenarios for the LHCb experiment", LHC Project Report 1009", CERN, Geneva (2007).
- [24] D. Banfi et al., "Beam-Beam Effects: Dynamical Aperture simulations summary", presentation at BEAM-BEAM Working Group 20th April 2015, CERN Geneva.
- [25] D. Banfi et al., "Beam-Beam Effects for Round versus Flat optics: Dynamical Aperture Simulations", presentation at the 4th Joint HiLumi LHC-LARP Annual Meeting, 17-21 November 2014, KEK, Japan.
- [26] J. Barranco and T. Pieloni, "Long-range beam-beam effects: Round versus Flat optics impact on dynamic aperture.", CERN-ACC-NOTE-2017-XXX (2017).
- [27] K. Hirata, "Beam-beam interaction with a crossing angle", KEK Preprint 93-190.
- [28] A. Piwinski, DESY Report DESY 77/18 (1977).
- [29] L. H. A. Leunissen, F. Schmidt and G. Ripken, "Six-dimensional beam-beam kick including coupled motion", PRSTAB, Volume 3, 124002 (2000).
- [30] J. Barranco and T. Pieloni, "Open Questions regarding SixTrack BB 6D lens", Beam-beam and luminosity meeting, 24 March 2014.
- [31] K. Yokoya et al., "Tune Shift of Coherent Beam-Beam Oscillations", KEK Preprint 89-14 (1989); Particle Accelerators, v.27, p.181 (1990).

Appendices

A Technical details

All optics files (Tab: A.1) and error map (Tab: A.2) files used in the simulation shown in this note are available in `/afs/cern.ch/eng/lhc/optics`.

Table A.1: Optics files for round and flat beams.

Optics version	β^* in IR1/5 (m)	β^* in IR2/8 (m)	Optics file
Round Optics			
SLHCV3.1b	0.4	10	opt_0400_0400thin.madx
SLHCV3.1b	0.33	10	opt_0330_0330thin.madx
SLHCV3.1b	0.15	10	opt_0150_0150thin.madx
SLHCV3.1b	0.10	10	opt_0100_0100thin.madx
HLLHCV1.0	0.15	3	opt_round_thin.madx
Flat Optics			
SLHCV3.1b	0.05 – 0.2	10	opt_0050_0200thin.madx
SLHCV3.1b	0.075 – 0.3	10	opt_0075_0300thin.madx
SLHCV3.1b	0.4 – 0.1	10	opt_0400_0100thin.madx
SLHCV3.1b	0.4 – 0.2	10	opt_0400_0200thin.madx
SLHCV3.1b	0.4 – 0.3	10	opt_0400_0300thin.madx

Table A.2: Error table for all error family taken into account into the simulation

Optics version	Magnet Family	Error Table
SLHCV3.1b	IT	errors/IT_errortable_v3
SLHCV3.1b	D1	errors/D1_errortable_v1
SLHCV3.1b	D2	errors/D2_errortable_v1
SLHCV3.1b	Q4	errors/Q4_errortable_v1
SLHCV3.1b	Q5	errors/Q5_errortable_v0
HLLHCV1.0	IT	errors/IT_errortable_v3_spec
HLLHCV1.0	D1	errors/D1_errortable_v1_spec
HLLHCV1.0	D2	errors/D2_errortable_v5_spec
HLLHCV1.0	Q4	errors/Q4_errortable_v1_spec
HLLHCV1.0	Q5	errors/Q5_errortable_v0_spec

B Simulation tools development and checks

The simulations presented are done with the SixTrack code [5]. SixTrack is a 6-dimensional symplectic code that is commonly used at CERN to characterize the dynamic aperture (DA) of the beams. The DA is the figure of merit used to characterize the strenght of the non-linearities of an accelerator and a large value of DA ensures the particle long term stability while circulating in the accelerator. At collision the DA is almost uniquely driven by the beam-beam interactions head-on at the Interaction Points (IPs) and long-range left and right of the IPs. So an accurate model of this lens is needed to properly model the physics. SixTrack allows two different models for the beam-beam lens: a 4D based on the Bassetti-Erskine [7] formalism and a 6D one including the bunch length effect based on Hirata's map [6, 27]. Until the second model was available all previous studies relied on the work of Piwinski [28] where that effect was considered negligible. The Sixtrack code is a so called weak-strong model, which means that a strong un-perturbed beam acts as a static lens while the opposite beam is studies as single particles. Particles at different amplitudes are tracked trough the accelerators and encounter the strong beam force which changes it's dynamics.

The 6D beam-beam lens was included in SixTrack at the beginning of the 2000 [29], however it was not routinely used, so to our best knowledge these are the first simulations with SixTrack and 6D beam-beam lens. Of course, a test and debugging process was required in order to gain confidence on the code model and to further modify it to allow for a full crab crossing scheme as required by the HL-LHC project. In order to simulate this case in SixTrack a modification was needed when boosting the strong beam. An additional variable θ_2 to control the strong beam was added in the plane of the crab crossing (namely x internally in SixTrack). All coordinates refereed to the strong are noted with \dagger .

$$\begin{aligned}
X^\dagger &= Z^\dagger \cos \alpha \sin \theta_2/2, & P_X^\dagger &= 0, & Y^\dagger &= Z^\dagger \sin \alpha \sin \theta/2, \\
P_Y^\dagger &= 0, & P_Z^\dagger &= 0, & \Sigma_{xx}^\dagger &= \Sigma_{xx}, \\
\Sigma_{xpxp}^\dagger &= \frac{1}{\cos^2 \theta_2/2} \Sigma_{xpxp}, & \Sigma_{yy}^\dagger &= \Sigma_{yypyp}, & \Sigma_{yypyp}^\dagger &= \frac{1}{\cos^2 \theta/2} \Sigma_{yypyp}, \\
\Sigma_{xxp}^\dagger &= \frac{1}{\cos \theta_2/2} \Sigma_{xxp}, & \Sigma_{xy}^\dagger &= \Sigma_{xy}, & \Sigma_{xyp}^\dagger &= \frac{1}{\cos \theta/2} \Sigma_{xyp}, \\
\Sigma_{xpy}^\dagger &= \frac{1}{\cos \theta_2/2} \Sigma_{xpy}, & \Sigma_{xpyyp}^\dagger &= \frac{1}{\cos^2 \theta_2/2} \Sigma_{xpyyp}, & \Sigma_{yyp}^\dagger &= \frac{1}{\cos \theta/2} \Sigma_{yyp}
\end{aligned} \tag{B.1}$$

Equation (B.1) shows how the second order matrix of the strong beam would like in the case of crab crossing ($\theta_2 = 0$). In addition during the set up of the 6D beam-beam interaction simulations a bug was found in the case of reading external beam sizes for the case of flat beams. The 6D beam-beam lens calculates the collision at the different slices by transporting the beam sizes from the interaction point (IP) to the actual collision point (CP). Since in the modification done to read the beam sizes from the fort.2 file only Σ_{xx} and Σ_{yy} were updated, it was not possible to transport longitudinally to the rest CPs and thus not taking into account the hour-glass effect. This resulted in a overestimated kick [30]. The 6D beam-beam routines were modified to allow calculate the second order matrix for given optics.

$$\begin{aligned}
\Sigma_{xx}^\dagger(S) &= \Sigma_{xx}^\dagger(0) + 2\Sigma_{xpxp}^\dagger(0)S + \Sigma_{xpxp}^\dagger(0)S^2 \\
\Sigma_{yy}^\dagger(S) &= \Sigma_{yy}^\dagger(0) + 2\Sigma_{yypyp}^\dagger(0)S + \Sigma_{yypyp}^\dagger(0)S^2 \\
\Sigma_{xy}^\dagger(S) &= \Sigma_{xy}^\dagger(0) + [\Sigma_{xyp}^\dagger(0) + \Sigma_{xpy}^\dagger(0)]S + \Sigma_{xpyyp}^\dagger(0)S^2
\end{aligned} \tag{B.2}$$

Equation (B.2) shows how the beam sizes are transported from the IP ($S = 0$) to each of the collision points (S), defined as $S = \frac{Z^\dagger - z_i}{2}$ with z_i the longitudinal position of each particle within the bunch and Z^\dagger the longitudinal position of each strong beam slice.